

AN ATTRIBUTION ANALYSIS OF CHANGES IN POTENTIAL EVAPOTRANSPIRATION IN THE BEIJING–TIANJIN–HEBEI REGION UNDER CLIMATE CHANGE

YU Zhan-jiang (于占江)^{1,2}, ZHOU Wei-can (周伟灿)¹, ZHANG Xiao (张 晓)³

(1. Nanjing University of Information Science and Technology, Nanjing 210044 China;

2. Shijiazhuang Meteorological Bureau, Shijiazhuang 050081 China;

3. College of Resources and Environment, Shijiazhuang University, Shijiazhuang 050035 China)

Abstract: Based on the measurements obtained at 64 national meteorological stations in the Beijing-Tianjin-Hebei (BTH) region between 1970 and 2013, the potential evapotranspiration (ET_0) in this region was estimated using the Penman-Monteith equation and its sensitivity to maximum temperature (T_{max}), minimum temperature (T_{min}), wind speed (V_w), net radiation (R_n) and water vapor pressure (P_{wv}) was analyzed, respectively. The results are shown as follows. (1) The climatic elements in the BTH region underwent significant changes in the study period. V_w and R_n decreased significantly, whereas T_{min} , T_{max} and P_{wv} increased considerably. (2) In the BTH region, ET_0 also exhibited a significant decreasing trend, and the sensitivity of ET_0 to the climatic elements exhibited seasonal characteristics. Of all the climatic elements, ET_0 was most sensitive to P_{wv} in the fall and winter and R_n in the spring and summer. On the annual scale, ET_0 was most sensitive to P_{wv} , followed by R_n , V_w , T_{max} and T_{min} . In addition, the sensitivity coefficient of ET_0 with respect to P_{wv} had a negative value for all the areas, indicating that increases in P_{wv} can prevent ET_0 from increasing. (3) The sensitivity of ET_0 to T_{min} and T_{max} was significantly lower than its sensitivity to other climatic elements. However, increases in temperature can lead to changes in P_{wv} and R_n . The temperature should be considered the key intrinsic climatic element that has caused the "evaporation paradox" phenomenon in the BTH region.

Key words: Beijing-Tianjin-Hebei region; climate change; potential evapotranspiration; climatic element; sensitivity coefficient

CLC number: P467 **Document code:** A

doi: 10.16555/j.1006-8775.2019.01.008

1 INTRODUCTION

As an important component of the hydrological cycle, evapotranspiration processes reflect the intensity of land interactions with the atmosphere (Atsumu and Martin^[1]; Chen et al.^[2]; Wang et al.^[3]). Rosenberg et al. found that a high proportion (60% -70%) of annual precipitation returns to the atmosphere through evapotranspiration^[4]. According to the Fifth Assessment Report of the Intergovernmental Panel on Climate Change, globally, the land surface temperature increased, on average, by approximately 0.85 °C between 1980 and 2012, making this period the hottest 30 years in the past 1,400 years (IPCC^[5]). Global warming has a significant impact on the hydrological cycle, and evapotranspiration is the main factor that affects regional and global water and heat balance calculations and is also an important index for evaluating the impact of global change on

hydrological and water resources (Xu et al.^[6]; Hesse et al.^[7]). Due to the lack of observed data of evapotranspiration, the potential evapotranspiration (ET_0) is often used to estimate the actual evapotranspiration based on the Penman-Monteith equation (Sentelhas et al.^[8]; Liu and Zhang^[9]).

Under the background of global warming, most pan evaporation (PE) values and calculated values of ET_0 in various locations around the globe have been decreasing in the past half-century (Peterson et al.^[10]; Cohen et al.^[11]; Gong et al.^[12]; Xu et al.^[13]; Shahzada et al.^[14]). Roderick and Farquhar referred to the climate-related hydrological phenomenon of simultaneous occurrences of increases in temperature and decreases in ET_0 as the "evaporation paradox", which has garnered extensive attention^[15]. By analyzing the ET_0 from the land surface in China, Liu and Zhang noted a widespread "evaporation paradox" phenomenon in China on a watershed scale^[9]. Researchers around the world mostly attribute the "evaporation paradox" phenomenon to increases in air humidity, decreases in solar radiation (R_s), decreases in land surface V_w and increases in atmospheric aerosols (Liu et al.^[9]; Xu et al.^[13]; Stanhill and Cohen^[16]; Liang et al.^[17]; Yin et al.^[18]). Hupet and Vanclooster found a decreasing trend in the ET_0 in Belgium and that the ET_0 in this region was most sensitive to T_{max} ^[19]. Sumner and Jacobs believed that there

Received 2017-07-02; **Revised** 2018-10-18; **Accepted** 2019-02-15

Foundation item: National Natural Science Foundation of China (41475054)

Biography: YU Zhan-jiang, Ph. D., primarily undertaking research on weather forecasting, rainstorm and water resource.

Corresponding author: ZHANG Xiao, e-mail: zhangxiao7990@163.com

is a complementary relationship between PE and the actual evaporation from the land surface, i.e., when there is an increase in the actual evaporation from the land surface, there will be an increase in the amount of atmospheric water vapor in the evaporation pan environment, which will inhibit evaporation from the evaporation pan surface^[20]. Roderick and Farquhar believed that increases in cloud cover and aerosols led to a decrease in the total R_s , which in turn resulted in a decrease in the observed evaporation^[21]. The aerosol pollution over the BTH region was getting worse, which has affected the radiation and energy budget of the earth, and then altered the global climate. (Jacobson et al.^[22]; Park et al.^[23]; Zhang et al.^[24]). In addition, the Beijing-Tianjin-Hebei (BTH) region has a vulnerable ecological environment. Water resources are the core ecological problem in this region. Currently, the carrying capacity of water resources in the BTH region exceeds the warning limit, and the resultant detrimental risk to industrial and agricultural production is more prominent than in the past. However, few studies facilitate a quantitative investigation of the impact of climate change on the hydrological cycle of ET_0 in the BTH region.

In this study, the ET_0 in the BTH region was calculated using the Penman-Monteith equation, and the sensitivity of ET_0 in this region to such climatic elements as maximum temperature (T_{max}), minimum temperature (T_{min}), water vapor pressure (P_{wv}), wind speed (V_w) and net radiation (R_n) was analyzed with an aim to determine the intrinsic element that causes changes in ET_0 .

2 DATA AND METHODS

2.1 Data

The meteorological data used in this study were obtained from the Sharing Service Platform of the China Meteorological Data Service Center (<http://data.cma.cn/>) and consisted of data acquired at 64 national standard meteorological stations in the BTH region, including daily mean temperature, T_{max} , T_{min} , V_w at 10 m above the ground, sunshine duration (S) and relative humidity. The 20-cm PE data acquired at 38 stations between 1970 and 2013 were used to assess the accuracy of the ET_0 calculated using the Penman-Monteith equation. The characteristics of spatial changes in each parameter were obtained using the inverse distance weighted method. Fig.1 shows the spatial distribution of the observation stations.

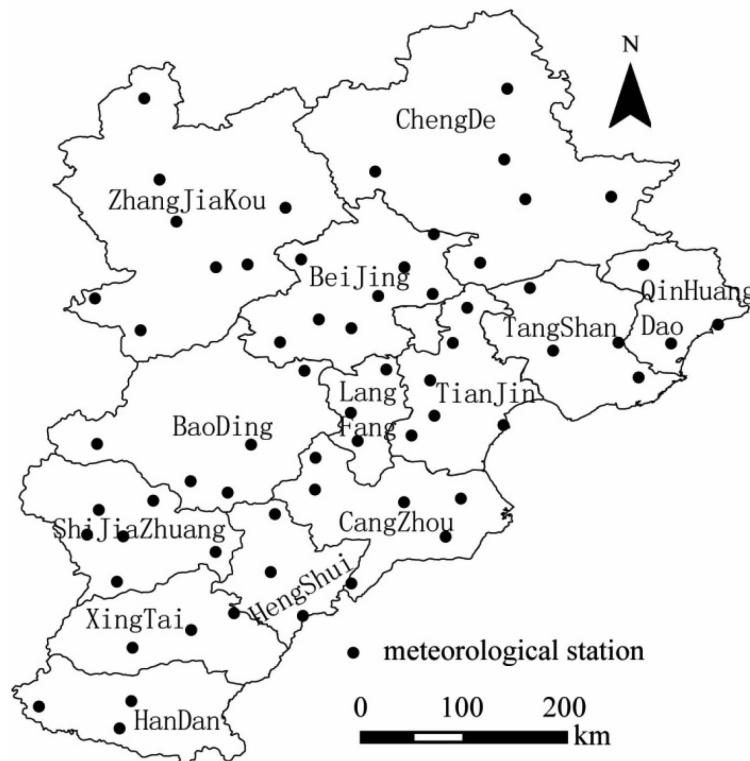


Figure 1. Distribution of meteorological stations in the BTH region.

2.2 Methods

2.2.1 ET_0

ET_0 refers to the maximum evapotranspiration capacity of the land surface in a region when there is an ample water supply, and it is an important component of surface water cycle and energy balances^[8]. ET_0 has been

extensively used in research on the management of water resources (e.g., farmland irrigation and calculations of the amounts of water needed by crops). In this study, the Penman-Monteith equation recommended by the Food and Agriculture Organization of the United Nations was used to calculate the ET_0 in the BTH region in a grassland

with a vegetation height of 0.12 m, a fixed surface resistance of 70 s/m and an albedo of 0.23 as the reference underlying surface^[9]. The Penman-Monteith equation is as follows:

$$ET_0 = \frac{0.408\Delta(R_n - G) + \gamma \frac{900}{T_{mean} + 273} U_2 (VP_s - VP)}{\Delta + \gamma(1 + 0.34U_2)} \quad (1)$$

where ET_0 is the potential evapotranspiration (mm); R_n is the net radiation of the crop surface ($MJ/(m^2 \cdot day)$); G is the soil heat flux ($MJ/(m^2 \cdot day)$); γ is the dry/wet constant ($kPa/^\circ C$); Δ is the slope of the saturated P_{wv} curve ($kPa/^\circ C$); VP_s is the mean saturated P_{wv} (kPa); VP is the actual P_{wv} (kPa); T_{mean} is the mean temperature ($^\circ C$); and U_2 is the V_w at 2 m above the ground (m/s). R_n is the sum of shortwave R_s and longwave land surface radiation (R_{ls}) and reflects the energy budget. The equation used to calculate R_n is as follows:

$$R_n = R_{rs} - R_{nl} \quad (2)$$

$$R_{rs} = (1 - \alpha)R_s \quad (3)$$

$$R_s = (a_s + b_s \frac{S}{N})R_a \quad (4)$$

$$R_{nl} = \sigma \left[\frac{T_{max,K}^4 + T_{min,K}^4}{2} \right] (0.34 - 0.14\sqrt{VP}) (1.35 \frac{R_s}{R_{so}} - 0.35) \quad (5)$$

where R_{rs} is the shortwave radiation ($MJ/(m^2 \cdot day)$); R_{nl} is the net outgoing longwave radiation ($MJ/(m^2 \cdot day)$); R_s is the solar radiation ($MJ/(m^2 \cdot day)$); S is the sunshine duration (h); N is the maximum sunshine duration (h); R_a is the solar radiation at the top of the atmosphere ($MJ/(m^2 \cdot day)$); $T_{max,K}$ and $T_{min,K}$ are the maximum and minimum absolute temperatures, respectively (K); σ is the Stefan-Boltzmann constant; and a , a_s and b_s are empirical parameters ($a=0.23$, $a_s=0.25$ and $b_s=0.5$).

2.2.2 CLIMATE SENSITIVITY COEFFICIENTS OF ET_0

To investigate the climate sensitivity coefficient of ET_0 , McCuen proposed an index^[25], which was widely used in the climate study (Liu et al.^[9]; Gong et al.^[12]; Djaman et al.^[26]). It is defined as the ratio of the rate of

change in ET_0 to the rate of change in the climatic element in question as follows^[25]:

$$S_x = \lim \left(\frac{\Delta E_0 / E_0}{\Delta x / x} \right) = \frac{\partial E_0}{\partial x} \cdot \frac{x}{E_0} \quad (6)$$

where S_x is the dimensionless sensitivity coefficient of ET_0 with respect to the climatic element x , and E_0 is the ET_0 . A positive sensitivity coefficient means that ET_0 increases as the climatic element increases, whereas a negative sensitivity coefficient means that ET_0 decreases as the climatic element increases. In this study, the sensitivity of ET_0 to T_{min} , T_{max} , V_w , R_n and P_{wv} was discussed separately.

2.2.3 ALONG TIME TREND ANALYSES METHOD

The data loss and exceptions has an impact on the statistical result, therefore the Sen's slope methods was used to analyze the tendency. A big disadvantage to this approach, however, is that it was incapable of testing statistical significance (Kahya and Kalayci^[27]). Being able to test the statistical significance, the Mann-Kendall method is nonparametric and extensively used in the hydrological and meteorological fields (Sun et al.^[28]). The advantages of the Mann-Kendall test lie in that it does not require the samples to follow a certain distribution, and it is also not disturbed by a small number of anomalies. In the paper, the climate trend was studied by combination of the Sen's slope and Mann-Kendall method.

3 RESULTS AND ANALYSIS

3.1 Estimation based on the Penman -Monteith equation

To investigate the relationship of the PE value and the ET_0 in the BTH region, the correlation coefficient (R^2) between the PE data and the estimated values of ET_0 was calculated in the Fig.2. As shown is the figure, there is positive relationship between the PE data and the estimated values of ET_0 , and the correlation coefficient (R^2) is 0.71, passing the 95% significant level test. This result suggests that the ET_0 estimated can be well used with the Penman-Monteith equation to reflect the regional evaporation capacity.

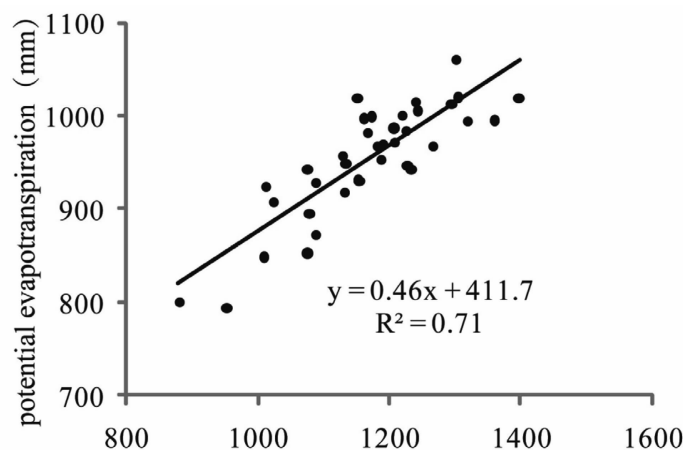


Figure 2. Relationship between ET_0 and PE data.

3.2 Changes in each climatic element and ET_0 in the BTH region

As shown by the distribution of their trend rates (Fig.3), all the climatic elements in the BTH region underwent significant changes from 1970 to 2013. The trend rates of the T_{\min} dropped off gradually from south to north (Fig.3a). A primarily increasing trend at a mean rate of $0.43\text{ }^{\circ}\text{C}/10\text{a}$ was found for T_{\min} in the study area. A statistical analysis showed that of the 64 meteorological stations in the study area, 59 stations passed the Mann-Kendall test at the 0.05 significance level in the increasing trend of T_{\min} . In addition, of the five stations where the recorded T_{\min} exhibited a decreasing trend, Chengde was only the station that passed the Mann-Kendall test at the 0.05 significance level. An increasing trend at a mean rate of $0.2\text{ }^{\circ}\text{C}/10\text{a}$ was found for T_{\max} in the BTH region, which gradually became less prominent from north to south, with the increasing trend of T_{\max} in Zhangjiakou being the most prominent (Fig.3b). The V_w in the study area exhibited a decreasing trend at a rate of $0.13\text{ m}/(\text{s}\cdot 10\text{a})$ in the past 45 years. The V_w recorded at all the stations decreased over the years, except for the Chengde and Fengning stations, where the recorded V_w increased (Fig.3c). The decreasing trends of V_w recorded at 53

stations passed the Mann-Kendall test at the 0.05 significance level. The decreasing trend rate for V_w at the Zhangbei station was the highest, at $0.43\text{ m}/(\text{s}\cdot 10\text{a})$. A significant decreasing trend was apparent for S in the BTH region. The decreasing trends of S recorded at 60 stations passed the Mann-Kendall test at the 0.05 significance level. The mean climatic trend rate for S in the entire region was $-2.57\text{ h}/10\text{a}$. The climatic decreasing trend rate for S recorded at the Miyun station was the highest, at $5.41\text{ h}/10\text{a}$. Decreases in S mostly occurred in Beijing, Tianjin, Shijiazhuang, Xingtai and Handan (Fig.3d). A significant trend can be found for P_{ww} in the region. Of the 46 stations where the P_{ww} increased, 14 stations passed the Mann-Kendall test at the 0.05 significance level (Fig.3e). The mean climatic trend rate for P_{ww} in the entire region was $0.04\text{ hPa}/10\text{a}$. As a result of the changes in S, T_{\max} , T_{\min} and P_{ww} , the R_n in the entire region also underwent significant changes. The spatial distribution of R_n was the same as that of S (Fig.3f). Most significant decreases in R_n occurred in Beijing and Tianjin as well as the north of Shijiazhuang. The climatic trend rate for R_n was $-0.13\text{ (MJ/m}^2\cdot\text{d)}/10\text{a}$. Of all the stations, an increasing trend was only apparent for R_n recorded at the Changli station, which also passed the Mann-Kendall test at the 0.05

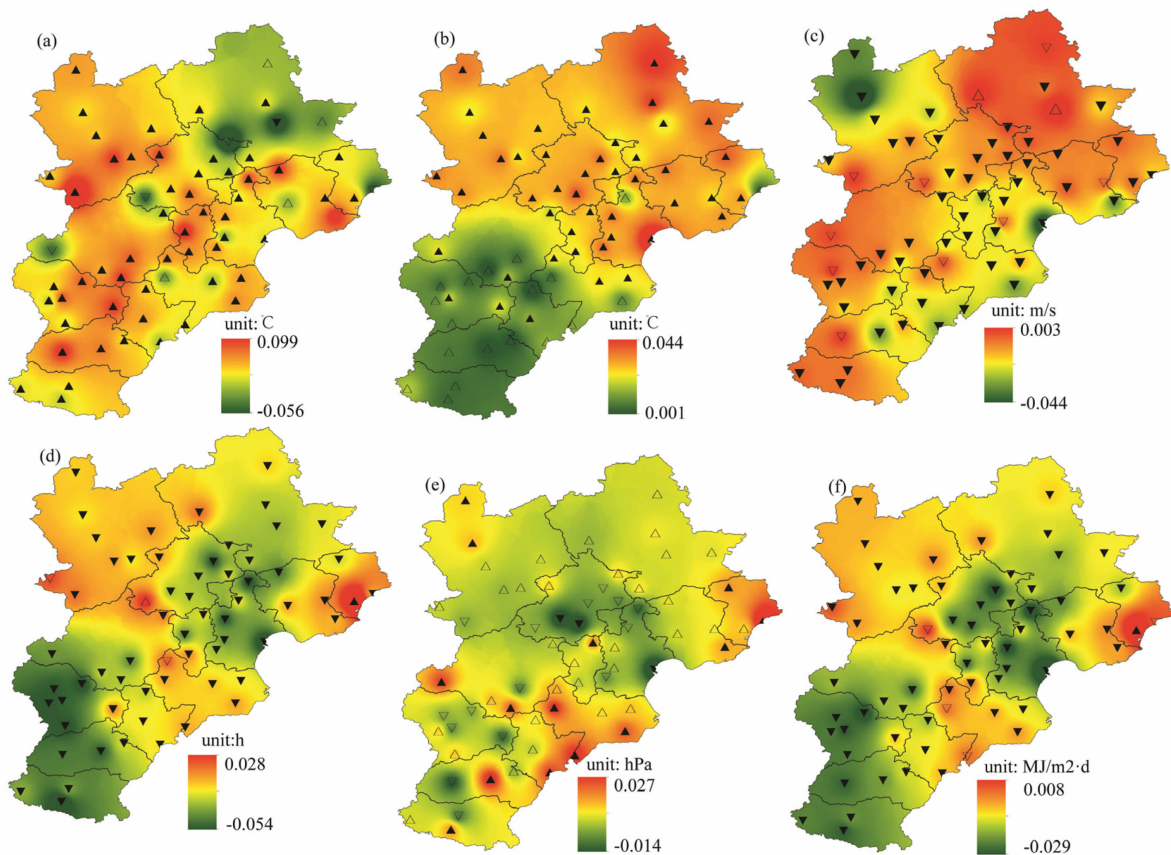


Figure 3. Distribution of the trend rates of the climatic elements in the BTH region (a: T_{\min} ; b: T_{\max} ; c: V_w ; d: S; e: P_{ww} ; f: R_n ; \triangle signifies that the increasing trend failed to pass the Mann-Kendall test at the 0.05 significance level; \blacktriangle signifies that the increasing trend passed the Mann-Kendall test at the 0.05 significance level; ∇ signifies that the decreasing trend failed to pass the Mann-Kendall test at the 0.05 significance level; \blacktriangledown signifies that the decreasing trend passed the Mann-Kendall test at the 0.05 significance level).

significance level. The decreasing trends of R_n at the 59 stations passed the Mann-Kendall test at the 0.05 significance level.

The ET_0 in the BTH region had a multi-year mean value of 950 mm, and it gradually decreased from southeast to northwest, with low-value areas mostly distributed in Chengde (Fig.4a). As a result of the changes in each climatic element, the ET_0 in the study area underwent significant changes. The ET_0 in the study area

mainly exhibited a decreasing trend (Fig.4b) at a mean rate of -12.16 mm/10a. The decreasing trends of ET_0 recorded at 57.8% of the stations passed the Mann-Kendall test at the 0.05 significance level, indicating a relatively widespread "evaporation paradox" phenomenon in the BTH region, which is in agreement with the decreasing trend of ET_0 in the Haihe River Basin found by Liu et al.^[9].

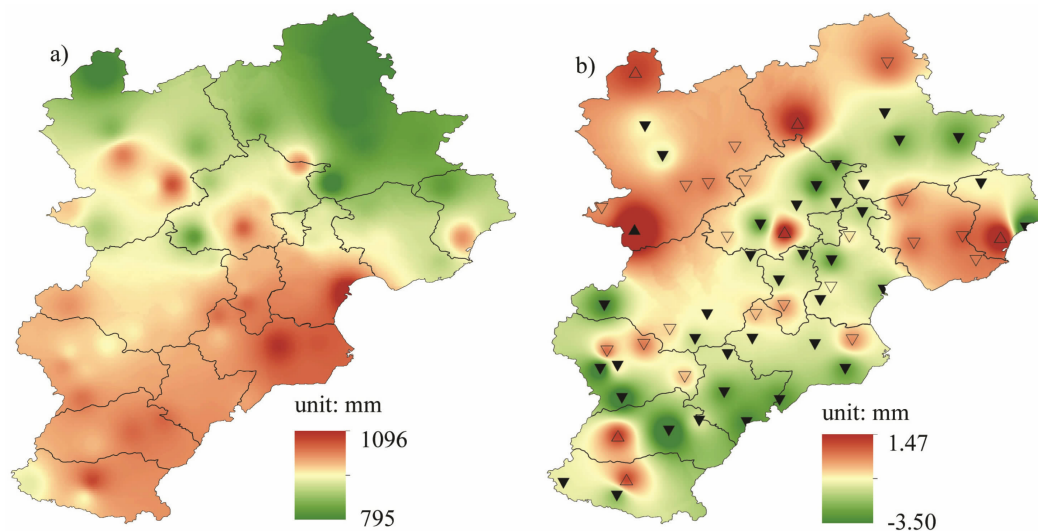


Figure 4. Distribution of multi-year mean ET_0 (a) and its trend rate (b) (\triangle signifies that the increasing trend failed to pass the Mann-Kendall test at the 0.05 significance level; \blacktriangle signifies that the increasing trend passed the Mann-Kendall test at the 0.05 significance level; ∇ signifies that the decreasing trend failed to pass the Mann-Kendall test at the 0.05 significance level; \blacktriangledown signifies that the decreasing trend passed the Mann-Kendall test at the 0.05 significance level).

3.3 Analysis of the sensitivity of ET_0 to each climatic element

Based on the monthly changes in the sensitivity coefficient of ET_0 with respect to each climatic element in the BTH region in the past 45 years (Fig.5), the sensitivity coefficients of ET_0 with respect to V_w and R_n had positive values, whereas the sensitivity coefficient of ET_0 with respect to P_{ww} had a negative value, indicating that the ET_0 in this region increased with an increasing V_w and R_n but decreased with an increasing P_{ww} . The sensitivity coefficient of ET_0 with respect to V_w ranged from 0.06 to 0.48, with the lowest values in August and highest values in December. The sensitivity coefficient of ET_0 with respect to R_n was from 0.26 to 0.84, with the highest values in August and lowest values in December. The sensitivity coefficient of ET_0 with respect to P_{ww} was from -0.29 to -1.15 , with the lowest sensitivity in April and the highest sensitivity in December. The sensitivity coefficient of ET_0 with respect to T_{min} ranged from -0.05 to 0.18 and decreased with an increasing T_{min} in the winter. The sensitivity coefficient of ET_0 with respect to T_{max} ranged from -0.01 to 0.22. The highest sensitivity of ET_0 to both T_{min} and T_{max} occurred in August.

There is a significant seasonal difference in the

sensitivity coefficient of ET_0 with respect to each climatic element (Table 1). In the spring, ET_0 was most sensitive to R_n , followed by P_{ww} , V_w , T_{max} and T_{min} . In the summer, ET_0 was most sensitive to R_n , followed by P_{ww} , T_{max} , T_{min} and V_w . In the fall, ET_0 was most sensitive to P_{ww} , followed by R_n , V_w , T_{max} and T_{min} . In the winter, ET_0 was most sensitive to P_{ww} , followed by V_w , R_n , T_{max} and T_{min} . On the annual scale, ET_0 was most sensitive to P_{ww} , followed by R_n , V_w , T_{max} and T_{min} .

Table 1. Seasonal statistics of the sensitivity coefficient of ET_0 with respect to each climatic element.

Tests	V_w	T_{min}	T_{max}	R_n	P_{ww}
Spring	0.22	0.01	0.07	0.56	-0.33
Summer	0.10	0.13	0.17	0.79	-0.57
Fall	0.25	0.04	0.08	0.57	-0.87
Winter	0.40	-0.02	0.01	0.34	-0.90
Annual mean	0.24	0.04	0.08	0.57	-0.67

Figure 6 shows the spatial distribution of the sensitivity of ET_0 in the BTH region to each climatic element. As demonstrated in Fig.6, there is inconsistency

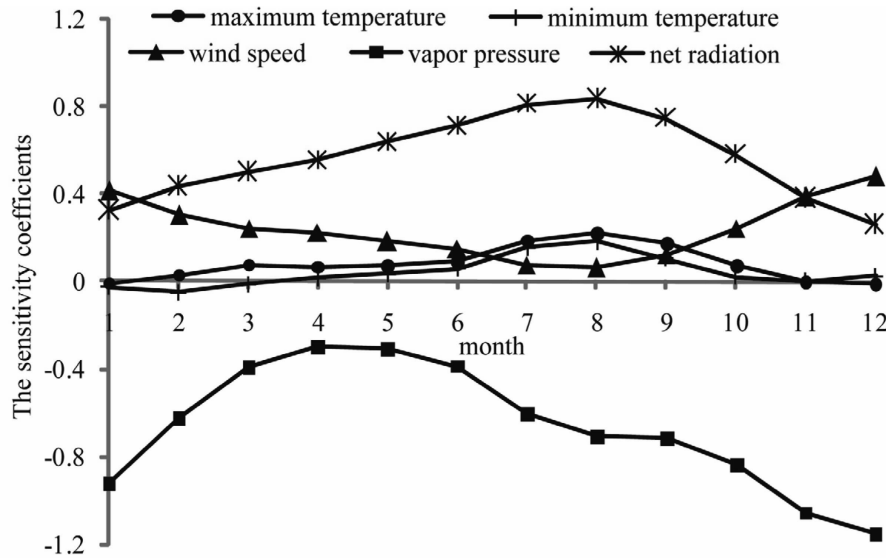


Figure 5. Monthly changes in the sensitivity coefficients of ET_0 with respect to climatic elements.

in the spatial distribution of the sensitivity coefficients of ET_0 with respect to the climatic elements. The sensitivity coefficient of ET_0 with respect to T_{min} ranged from -0.03 to 0.07 . The sensitivity coefficient of ET_0 with respect to T_{min} had a negative value for all the areas, except for Kangbao and Zhangbei. The distribution of the effects of T_{max} on ET_0 was inconsistent with the distribution of the effects of T_{min} on ET_0 . The sensitivity coefficient of ET_0 with respect to T_{max} had a positive value ($0.01-0.15$) for all the areas, indicating that increases in T_{max} were favorable to increases in ET_0 . Chengde is the area where the ET_0 was most sensitive to T_{max} , with a sensitivity coefficient of 0.12 (Table 2). ET_0 increased with an increasing V_w . The sensitivity coefficient of ET_0 with respect to V_w ranged from 0.18 to 0.31 . The areas where ET_0 was highly sensitive to V_w were mainly concentrated in Zhangjiakou and Beijing as well as the junction of Beijing and Chengde. The sensitivity coefficient of ET_0 with respect to P_{wv} ranged from -0.85 to -0.39 . ET_0 decreased with an increasing P_{wv} . ET_0 was the least sensitive to the changes in P_{wv} in Zhangjiakou. The sensitivity coefficient of ET_0 with respect to R_s ranged from 1.18 to 2.37 . The sensitivity of ET_0 to R_s gradually increased from south to north. In comparison, the sensitivity coefficient of ET_0 with respect to R_n ranged from 0.45 to 0.67 . Due to the effects of P_{wv} and temperature, the sensitivity coefficient of ET_0 with respect to R_s was significantly greater than that with respect to R_n .

In addition, an increasing trend at a rate of $0.003/10a$, $0.004/10a$, $0.048/10a$ and $0.009/10a$ was also evident for the sensitivity coefficients of ET_0 with respect to V_w , T_{min} , R_n and P_{wv} , respectively, in the BTH region between 1970 and 2013. Except for V_w , the increasing trends of the sensitivity coefficients of ET_0 with respect to all the climatic elements passed the Mann-Kendall test at the 0.05 significance level. The sensitivity of ET_0 to T_{max} in the study area exhibited a decreasing trend at a rate of

$-0.002/10a$. This decreasing trend failed to pass the Mann-Kendall test at the 0.05 significance level.

3.4 Discussion

Under a general background of global warming, there is a notable "evaporation paradox" phenomenon in the BTH region, where decreases in V_w and R_s , and increases in P_{wv} contribute, to varying degrees, to the decrease in ET_0 . While its sensitivity coefficient with respect to temperature had a positive value, the sensitivity of ET_0 to temperature was significantly lower than its sensitivity to other climatic elements. Nevertheless, the effects of increases in temperature on ET_0 cannot be overlooked. An analysis of the correlation between ET_0 and its sensitivity coefficient with respect to each climatic element found that except for the correlation between ET_0 and its sensitivity coefficient with respect to T_{max} ($R^2=0$).

Table 2. Sensitivity coefficient of ET_0 in the BTH region with respect to each climatic element.

Administrative region	V_w	T_{min}	T_{max}	R_n	P_{wv}
Baoding	0.24	0.05	0.09	0.59	-0.73
Beijing	0.26	0.06	0.08	0.54	-0.61
Cangzhou	0.24	0.03	0.07	0.55	-0.69
Chengde	0.23	0.04	0.12	0.61	-0.69
Handan	0.21	0.05	0.11	0.63	-0.75
Hengshui	0.22	0.04	0.09	0.59	-0.76
Langfang	0.25	0.04	0.07	0.56	-0.68
Qinhuangdao	0.24	0.05	0.10	0.57	-0.68
Shijiazhuang	0.23	0.05	0.09	0.61	-0.74
Tangshan	0.23	0.06	0.10	0.57	-0.72
Tianjin	0.26	0.04	0.06	0.53	-0.64
Xingtai	0.22	0.04	0.08	0.60	-0.75
Zhangjiakou	0.26	0.02	0.06	0.52	-0.48

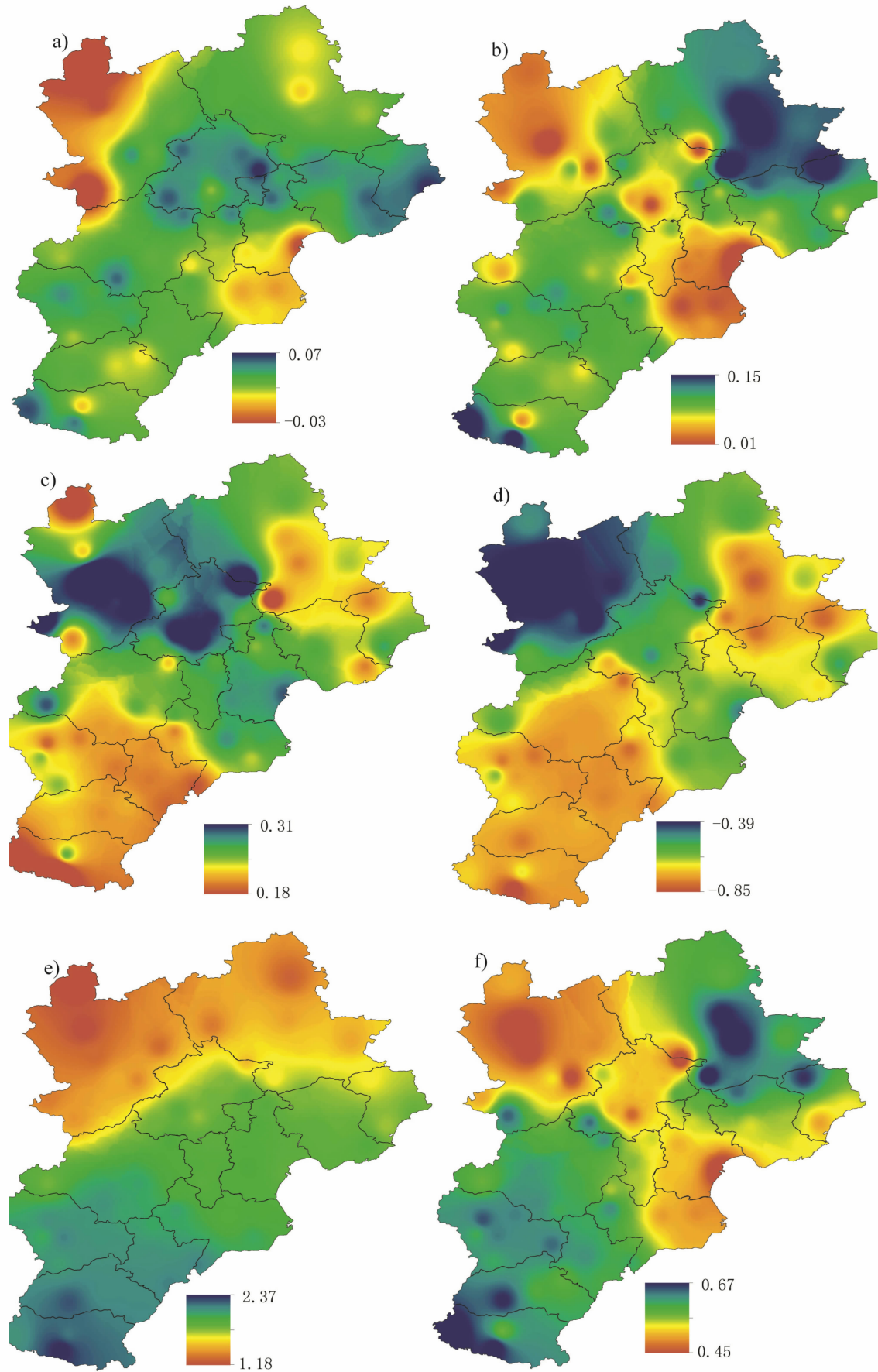


Figure 6. Spatial distribution of the sensitivity coefficients of ET_0 with respect to climatic elements (a: T_{min} ; b: T_{max} ; c: V_w ; d: P_w ; e: S ; f: R_n).

43), which passes the significance test at a 0.99 confidence level, the correlations between ET_0 and its sensitivity coefficients with respect to the climatic elements (V_w , R_s , P_{wv} and T_{min}) ($R^2 < 0.2$) all failed to pass the significance test at a 0.99 confidence level. In addition, the multiple R^2 between ET_0 and its sensitivity coefficients with respect to T_{min} , T_{max} and P_{wv} is 0.86. Moreover, the changes in the actual P_{wv} in the BTH region are significantly positively correlated with T_{max} , T_{min} and T_{mean} , with a $R^2 > 0.80$. This is mainly because of an increase in temperature that results in an increase in the amount of water vapor contained in the atmosphere, thereby leading to an increase in P_{wv} in the region.

The sensitivity coefficient of ET_0 with respect to R_n is only smaller than the sensitivity coefficient with respect

to P_{wv} . R_n is affected by R_{ns} and longwave R_{nl} . An increasing trend is apparent for longwave R_{nl} in the past 45 years (ellipsis figure), suggesting that the increase in longwave radiation caused by increases in temperature is greater than the decrease in longwave radiation caused by increases in P_{wv} . The decrease in R_{ns} caused by decreases in S and the increase in longwave R_{nl} caused by increases in temperature have together resulted in a decrease in the R_n of the land surface using formula 2–5. In addition, the R^2 between the sensitivity coefficient of ET_0 with respect to R_n and the sensitivity coefficients of ET_0 with respect to R_s , T_{max} and P_{wv} are 0.4, 0.85 and -0.84 , respectively (Fig.7). Thus, the intrinsic effects of R_n on ET_0 are significantly related to T .

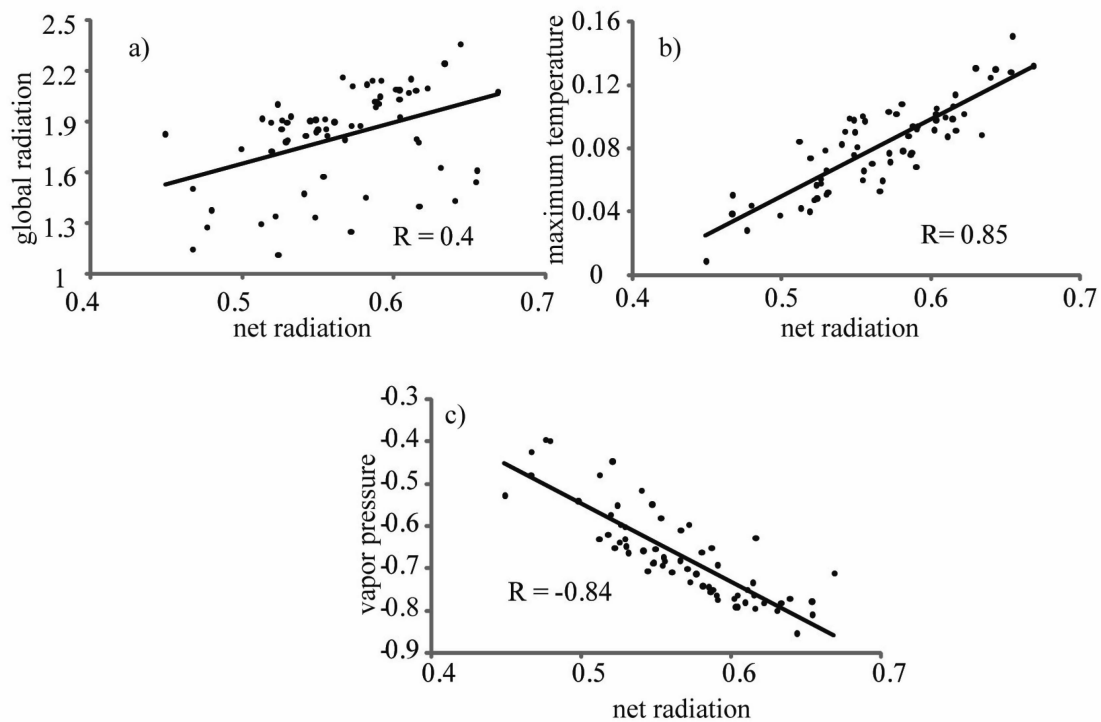


Figure 7. Relationships between the sensitivity coefficient of ET_0 with respect to R_n and the sensitivity coefficients of ET_0 with respect to R_s (a), T_{max} (b) and P_{wv} (c).

There is heavy aerosol pollution in the BTH region. Highly concentrated aerosol particles can affect climate change through direct and indirect radiation effects. The decrease in radiation caused by increases in cloud cover or atmospheric aerosols has been considered a main cause of decreases in PE^[15,21]. A further analysis based on more comprehensive observed data is necessary to determine the extent of the contribution of R_s and aerosol pollution to the occurrence of the "evaporation paradox" phenomenon in the BTH region.

4 CONCLUSIONS

To determine the characteristics of the response of the hydrological cycle in the BTH region to climate change, the changes in ET_0 were calculated based on the

daily data observed at 64 meteorological stations in this region between 1970 and 2013, and the characteristics of the sensitivity of ET_0 to each climatic element were also analyzed. The conclusions derived from this study are summarized as follows:

(1) Temperature, P_{wv} , V_w , S and R_n all underwent significant changes. T_{max} , T_{min} and P_{wv} increased significantly, whereas V_w , S and R_n decreased considerably. The ET_0 in the study area exhibits a decreasing trend at a mean rate of -12.16 mm/10a, suggesting a relatively widespread "evaporation paradox" phenomenon in the BTH region.

(2) There is a significant difference in the spatial distribution of the sensitivity of ET_0 to the climatic elements. Except for Kangbao and Zhangbei, two areas to

the north of Zhangjiakou, where the sensitivity coefficient of ET_0 with respect to T_{min} had a negative value, the sensitivity coefficient of ET_0 to T_{min} had a positive value for all the other areas. The sensitivity coefficients of ET_0 with respect to T_{max} , V_w and R_n each had a positive value, indicating that increases in each of these elements were favorable for increases in ET_0 . The sensitivity coefficient of ET_0 with respect to P_{ww} had a negative value for all the areas (-0.85 to -0.40) and decreased with an increasing P_{ww} .

(3) On an annual scale, ET_0 was most sensitive to P_{ww} , followed by R_n , V_w , T_{max} and T_{min} . There was a significant seasonal difference in the sensitivity coefficient of ET_0 with respect to each climatic element. ET_0 was most sensitive to R_n in the spring and summer and to P_{ww} in the fall and winter. In addition, a decreasing trend was evident for the sensitivity of ET_0 to T_{max} , whereas an increasing trend was apparent for the sensitivity of ET_0 to each of V_w , T_{min} , R_n and P_{ww} .

(4) In the BTH region, the sensitivity of ET_0 to T_{min} and T_{max} were significantly lower than that to V_w , R and P_{ww} . Nevertheless, the effects of increases in temperature on ET_0 cannot be overlooked. The "evaporation paradox" phenomenon in the BTH region should be attributed to increases in temperature.

REFERENCES:

- [1] ATSUMU O, MARTIN W. Is the hydrological cycle accelerating? [J] *Science*, 2002, 298(5597): 1345-1346.
- [2] CHEN S, LIU Y, THOMAS A. Climatic change on the Tibetan Plateau: Potential evapotranspiration trends from 1961-2000 [J]. *Clim Change*, 2006, 76(3-4): 291-319.
- [3] WANG Y J, LIU B, SU B D, et al. Trends of calculated and simulated actual evaporation in the Yangtze River Basin [J]. *J Clim*, 2011, 24(24): 4494-4507.
- [4] ROSENBERG N J, BLAD B L, VERMA S B, et al. *Microclimate: the biological environment* [M]. New York: Wiley Press, 1983.
- [5] IPCC: Climate change 2013. The physical science basis. contribution of Working Group I to the fifth assessment report of the Intergovernmental Panel on Climate Change [M]. Cambridge: Cambridge University Press, 2013.
- [6] XU C Y, GONG L, JIANG T, et al. Analysis of spatial distribution and temporal trend of reference evapotranspiration and pan evaporation in Changjiang (Yangtze River) catchment [J]. *J Hydrol*, 2006, 327: 81-93.
- [7] HESSE C, KRYSANOVA V, STEFANOVA A, et al. Assessment of climate change impacts on water quantity and quality of the multi-river Vistula Lagoon catchment [J]. *Int Assoc Sci Hydrol Bull*, 2015, 60(5): 890-911.
- [8] SENTELHAS P C, GILLESPIE T J, SANTOS E A. Evaluation of FAO Penman-Monteith and alternative methods for estimating reference evapotranspiration with missing data in Southern Ontario, Canada [J]. *Agricul Water Manage*, 2010, 97(5): 635-644.
- [9] LIU Chang-ming, ZHANG Dan. Temporal and spatial change analysis of the sensitivity of potential evapotranspiration to meteorological influencing factors in China [J]. *Acta Geogr Sinica*, 2011, 66 (5): 579-588 (in Chinese).
- [10] PETERSON T C, GOLUBEV V S, GROISMAN P Y. Evaporation losing its strength [J]. *Nature*, 1995, 377 (6551): 687-688.
- [11] COHEN S, IANETZ A, STANHILL G. Evaporative climate changes at Bet-Dagan, Israel, 1964-1998 [J]. *Agric Forest Meteorol*, 2002, 111(2): 83-91.
- [12] GONG L B, XU C Y, CHEN D, et al. Sensitivity of the Penman-Monteith reference evapotranspiration to key climatic variables in the Changjiang basin [J]. *J Hydrol*, 2006, 329(3-4): 620-629.
- [13] XU Y P, PAN S, FU G, et al. Future potential evapotranspiration changes and contribution analysis in Zhejiang Province, East China [J]. *J Geophys Res Atmos*, 2014, 119(5): 2174-2192.
- [14] SHAHZADA A, KALIM U, AZMAT H, et al. Meteorological impacts on evapotranspiration in different climatic zones of Pakistan [J]. *J Arid Land*, 2017, 9(6): 938-952.
- [15] RODERICK M L, FARQUHAR G D. Changes in New Zealand pan evaporation since the 1970s [J]. *Int J Climatol*, 2010, 25(15): 2031-2039.
- [16] STANHILL G, COHEN S. Global dimming: a review of the evidence for a widespread and significant reduction in global radiation with discussion of its probable causes and possible agricultural consequences [J]. *Agric Forest Meteorol*, 2001, 107(4): 255-278.
- [17] LIANG Li-qiao, LI Li-juan, ZHANG Li, et al. Sensitivity of Penman-Monteith reference crop evapotranspiration in Tao'er River basin of Northeastern China [J]. *Chin Geograph Sci*, 2008, 18(4): 340-347 (in Chinese).
- [18] YIN Y, WU S, CHEN G, et al. Attribution analyses of potential evapotranspiration changes in China since the 1960s [J]. *Theor Appl Climatol*, 2010, 101(1-2): 19-28.
- [19] HUPET F, VANCLOOSTER M. Effect of the sampling frequency of meteorological variables on the estimation of the reference evapotranspiration [J]. *J Hydrol*, 2001, 243(3): 192-204.
- [20] SUMNER D M, JACOBS J M. Utility of Penman-Monteith, Priestley-Taylor, reference evapotranspiration, and pan evaporation methods to estimate pasture evapotranspiration [J]. *J Hydrol*, 2005, 308(1-4): 81-104.
- [21] RODERICK M L, FARQUHAR G D. The cause of decreased pan evaporation over the past 50 years [J]. *Science*, 2002, 298(5597): 1410-1411.
- [22] JACOBSON M Z, KAUFMAN Y J, RUDICH Y. Examining feedbacks of aerosols to urban climate with a model that treats 3-D clouds with aerosol inclusions [J]. *J Geophys Res Atmos*, 2007, 112(D24): 1-18.
- [23] PARK R J, KIM M J, JEONG J I, et al. A contribution of brown carbon aerosol to the aerosol light absorption and its radiative forcing in East Asia [J]. *Atmos Environ*, 2010, 44(11): 1414-1421.
- [24] ZHANG B, WANG Y X, HAO J M. Simulating aerosol-radiation-cloud feedbacks on meteorology and air quality over eastern China under severe haze conditions in winter [J]. *Atmos Chem Phys Discussions*, 2014, 14 (19): 2387-2404.
- [25] MCCUEN R H. A sensitivity and error analysis of procedures used for estimating evaporation [J]. *Water Resour Bull*, 1974, 10(3): 486-498.

- [26] DJAMAN K, TABARI H, BALDE A B, et al. Analyses, calibration and validation of evapotranspiration models to predict grass-reference evapotranspiration in the Senegal River Delta [J]. *J Hydrol Regional Studies*, 2016, 8(C): 82-94.
- [27] KAHYA E, KALAYCL S. Trend analysis of stream flow in Turkey [J]. *J Hydrol*, 2004, 289(1-4): 128-144.
- [28] SUN Peng, ZHANG Qiang, CHEN Xiao-hong, et al. Spatio-temporal patterns of sediment and runoff changes in the Poyang Lake Basin and underlying causes [J]. *Acta Geograph Sinica*, 2010, 65(7): 828-840 (in Chinese).

Citation: YU Zhan-jiang, ZHOU Wei-can and ZHANG Xiao. An attribution analysis of changes in potential evapotranspiration in the Beijing-Tianjin-Hebei region under climate change [J]. *J Trop Meteor*, 2019, 25(1): 82-91.